Vol 18 No 5, May 2009
1674-1056/2009/18(05)/2096-05

Chinese Physics B

© 2009 Chin. Phys. Soc.
and IOP Publishing Ltd

Effects of optical interference and annealing on the performance of poly (3-hexylthiophene): fullerene based solar cells

You Hai-Long(游海龙)[a)b)] and Zhang Chun-Fu(张春福)[c)†]

[a)] *School Of Microelectronics, Xidian University, Xi'an* 710071, *China*
[b)] *Key Laboratory of Wide Band-Gap Semiconductor Materials and Devices, Xi'an* 710071, *China*
[c)] *Department of Electrical and Computer Engineering, National University of Singapore, Singapore* 117576

(Received 1 September 2008; revised manuscript received 24 November 2008)

In this paper, the effects of optical interference and annealing on the performance of P3HT:PCBM based organic solar cells are studied in detail. Due to the optical interference effect, short circuit current density (J_{SC}) shows obvious oscillatory behaviour with the variation of active layer thickness. With the help of the simulated results, the devices are optimized around the first two optical interference peaks. It is found that the optimized thicknesses are 80 and 208 nm. The study on the effect of annealing on the performance indicates that post-annealing is more favourable than pre-annealing. Based on post-annealing, different annealing temperatures are tested. The optimized annealing condition is 160^{o}C for 10 min in a nitrogen atmosphere. The device shows that the open circuit voltage V_{OC} achieves about 0.65V and the power conversion efficiency is as high as 4.0 % around the second interference peak.

Keywords: organic solar cell, optical interference, annealing
PACC: 8630J, 7360F, 7220J

1. Introduction

Solar cells have become more and more attractive as the demand for renewable energy sources increases. The biggest obstacle of the traditional inorganic solar cells, especially the crystalline silicon-based solar cells, is the high manufacturing cost. Due to the promising low cost, flexibility, ease of fabrication, etc, now more and more attention has been paid to organic solar cells.[1−5] Since the discovery of ultrafast charge transfer between polymer and fullerene materials,[6] the power conversion efficiency (PCE) for bulk heterojunction (BHJ) solar cells has been improved steadily, which makes it possible to put them into practical applications in the near future.

Usually, BHJ organic solar cells are composed of a blend layer of conjugated polymer as electron donor (D) and fullerene as electron accepter (A). During the drying process, the materials are phase-separated due to thermal demixing, thereby forming interpenetrating domains of D and A materials. Upon excitation by a photon, an excited state is formed, which in semiconducting conjugated polymers typically has a diffusion length of less than 10 nm. Then for a well blended layer, the length scales of D and A phases should be smaller than the exciton diffusion length, so that most of the generated excitons can be dissociated into free carriers before decay. The electric field in the device, generated between the cathode and the anode, will pull the free electrons and holes to their respective electrodes before recombination. This transport process restricts the total active layer thickness which has a typical thickness of about 100 nm.[7] Because poly (3-hexylthiophene) (P3HT) has a high hole mobility in the regioregular state (10^{-4} to 10^{-2} cm^2/(V·s)) and an absorption tail extending into the red region, it appears to be one of the most suitable conjugated polymers to date for BHJ solar cells.

Because the active layer is very thin in organic solar cells compared with the incident light wavelength, the optical interference effect will influence the absorption and then the short circuit current density (J_{SC}). In addition, for different active layer thicknesses, the corresponding carrier transport processes are also different.[8] Then, the device performance depends on thickness. It is also found that the performances of P3HT:PCBM based devices can be greatly improved by annealing. After annealing,

†Corresponding author. E-mail: Zhangchunfu@nus.edu.sg

J_{SC} and fill factor (FF) have been observed to obviously increase.[9−13] However, the performance enhancement is related to the annealing sequence (pre-annealing, which is the annealing before the deposition of Al cathode, and post-annealing which is the annealing of the whole completed solar cell) and annealing temperature. In the present study, the effects of optical interference effect and annealing on device performance are studied in detail. According to the simulated results based on the optical model, the thickness is optimized around the first and second optical interference peaks and the optimized thicknesses are found to be 80 and 208 nm, respectively. By comparing the post-annealing process with the pre-annealing process, it is found that the devices with the post-annealing show a higher PCE. Then different annealing temperatures are tested for the devices based on post-annealing to find the optimized conditions. The optimized device shows that the PCE is as high as 4.0% around the second optical interference peak.

2. Experiment

The solar cells are composed of a layer of P3HT:PCBM thin film sandwiched between the anode and the cathode. Firstly, the indium tin oxide (ITO)-coated glass substrates were treated sequentially with detergent, de-ionized water, acetone, and isopropanol in an ultrasonic bath each for about 15 min. Then after treating the substrates by oxygen plasma for about 3 min, a 50 nm thin layer of poly (3, 4-ethylenedioxythiophene) (PEDOT): poly (styrenesulfonate) (PSS) was spin coated on the cleaned ITO glass substrates. After baking the PEDOT:PSS film at 120 °C for about 1 h in ambient conditions, the substrates were transferred into the glovebox. The P3HT:PCBM was dissolved in dichlorobenzene at a weight ratio of 1:0.8 and stirred for more than 72 h in the glove box before spin casting to form the blend layer. The blend layer thickness was controlled by changing the spin speed and solution concentration. Finally an Al electrode of about 100 nm in thickness was deposited by e-beam evaporation at a pressure of 2.4×10^{-4} Pa through a shadow mask. No buffer layer between the organic layer and cathode was used. The current–voltage (I–V) curves were measured by a Keithley 2400 source-measure unit in the dark and under air mass (AM) 1.5 solar illumination at intensity of 100 mW/cm^2. Absorption spectra of organic films on glass substrates were measured by a Shimadzu UV-3101 PC UV–VIS–NIR spectrophotometer.

3. Results and discussion

3.1. Pre-annealing and post-annealing

To compare the effect of the annealing process on the performance of the photovoltaic device, three types of solar cells were fabricated in an identical manner except for the annealing conditions. They are devices without annealing, with pre-treatment annealing and post-production annealing, separately. The typical I–V curves are plotted in Fig.1.

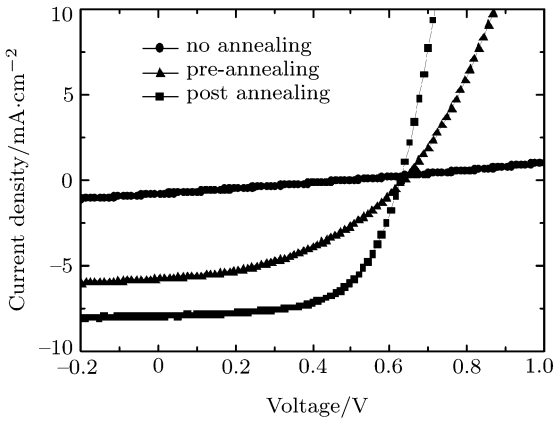


Fig.1. I–V characteristics of the photovoltaic cells ITO/PEDOT:PSS/P3HT:PCBM/Al under AM 1.5 illumination, with the P3HT:PCBM active layer thickness being about 80 nm and the photovoltaic cells annealed at 160 °C for 10 min.

The pre-annealed device and the post-annealed device exhibited an obvious increase in J_{SC} compared with the pristine device. The power conversion efficiency (PCE) was also greatly improved correspondingly. The pristine device only showed a PCE of 0.13%. However, after annealing, PCE went up to 1.58% for the pre-annealed device and 3.06% for the post-annealed device. Obviously, the post-annealed device showed the best performance. Compared with the pre-annealed device, the FF of the post-annealed device increased from 0.43 to 0.61. The increases in J_{SC} and FF implied a significant reduction in series resistance (R_s) of the solar cell. In fact, the value of R_s was reduced from 22.2 Ω·cm^2 for the pre-annealed device and further to 5.64 Ω·cm^2 for the post-annealed device.

Both annealing sequences can lead to the growing of P3HT and PCBM domains. This will induce the change of the device morphology. Before annealing,

the P3HT and PCBM domain sizes are very small and separated so that it is very difficult for electrons and holes to be collected by their corresponding electrodes efficiently. However, after annealing, with the P3HT and PCBM domains growing, an interpenetrating conduction network is formed, and the carriers can transport easily.[14] Then the carrier loss is reduced. This can be confirmed by the obvious increase of the J_{SC} and FF. However, the rapid PCBM diffusion is also the main limiting parameter in the blend films.[1,15] Too-fast PCBM diffusion rate will induce the formation of large PCBM aggregates in the P3HT:PCBM polymer blend and deteriorate the interpenetrating networks.[16] Charge generation and interfacial contact between P3HT and PCBM will most likely be reduced due to the overgrowth of PCBM.[15,16] Thus appropriate annealing should be performed to prevent the PCBM from overgrowing. In the pre-annealing devices, it is very easy for the PCBM domain to overgrow. However, in the post-annealed device, because of the confinement of the deposited Al film, the PCBM domain is relatively small. Smaller domain size implies that the overgrowing of the PCBM can be effectively prevented by overlaying an Al cathode. A better nanoscale control of the morphology can be promoted by prohibiting a too coarse phase segregation of PCBM molecules. A similar metal effect was also demonstrated on the organic surface by using a silver cap.[17] More efficient charge separation in the increased interfacial areas between P3HT and PCBM is believed to be one of the reasons for the improvement of the post-production annealed device. Because the post-annealed device shows the better performance, in the following, all the study is carried out under the post-annealing condition.

3.2. Optical interference effects and active layer thickness optimization

Theoretical analysis by using the optical model is a powerful way to understand and predict the performance of organic solar cells. The optical transfer matrix formalism (TMF) has been used in the optical model by us and other groups to predict J_{SC} of organic solar cells.[8−10] Here the same method is used to predict J_{SC} for the active layer thickness in a range from 50 to 250 nm. All the optical constants (n, k) of ITO, PEDOT:PSS, active layer are cited from the literature.[18,19] The results are plotted in Fig.2. Different from the J_{SC} of traditional Si based solar cells, J_{SC} here does not increase monotonically with layer thickness increasing due to optical interference effects and obviously oscillatory behaviour is observed. In conventional Si based solar cells, the active layer is usually thick and the optical interference effects can be neglected. However, for the organic solar cell, the active layer is usually only several hundred nanometres or even less than one hundred nanometres thick. This thickness is so thin compared with the wavelength, that the interference effects cannot be neglected any more. As shown in Fig.2, when the P3HT:PCBM ratio is 1:0.8, the first and second interference peaks are found at the P3HT:PCBM layer thicknesses of 85 and 230 nm. Thus work should be done around these two peaks to optimize the active layer thickness.

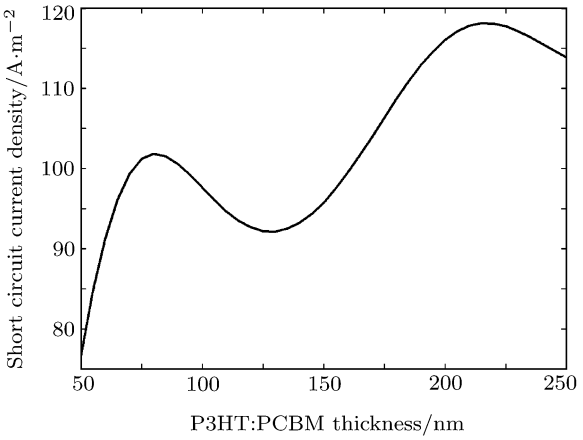


Fig.2. Short circuit current density versus P3HT:PCBM thickness with ratio P3HT:PCBM of 1:0.8 and device structure being composed of ITO/PEDOT:PSS/P3HT: PCBM/Al.

Figure 3 shows the experimental results for the active layer thickness optimization. As predicted, J_{SC} shows a periodic behaviour with the variation of the active layer thickness. The J_{SC} increases from 6.25 mA/cm^2 (for the device with active layer thickness $t = 64$ nm) to 6.93 mA/cm^2 (for $t = 80$ nm), and then decreases around the first interference peak. The same trend is observed around the second optical interference peak at a thickness of 208 nm. J_{SC} reaches a value as high as 10.37 mA/cm^2 at the second optical interference peak. The higher J_{SC} comes from the better absorption power. It is obviously shown that the second peak can absorb more light than the first peak as shown in Fig.4. Thus the second optical interference peak is more preferred to achieve a higher PCE. Then around this peak, the annealing conditions are investigated in the following part.

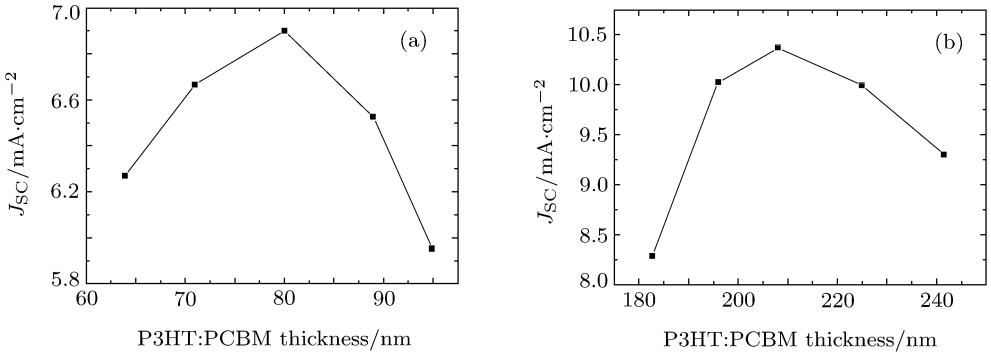


Fig.3. Optimization of active layer thickness around the first optical interference peak (a) and the second optical interference peak (b), measured from the devices that are post-annealed at 160 °C for 10 min.

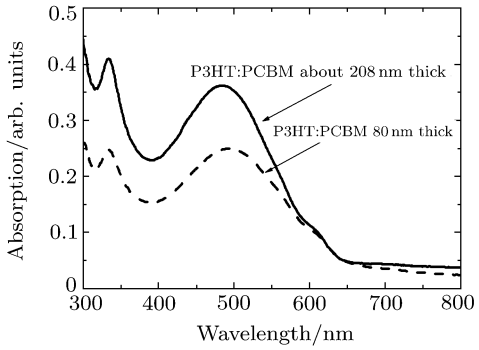


Fig.4. UV–visible absorption spectra of P3HT:PCBM (about 80 nm thick) and P3HT:PCBM (about 208 nm thick).

3.3. Optimization of annealing conditions

The device performance depends greatly on annealing conditions as seen from Fig.5. The reasons for the performance to be improved by the annealing process have been investigated.[9−13] It is clear that for an efficient organic BHJ solar cell, the D and A domains must be small enough so that most of the excitons can diffuse into the D/A interfaces before they decay. At the same time, the interpenetrating transport network must be formed for the efficient charge transport. Thus, the morphology optimization is of great importance. By varying the annealing conditions, the morphology can be well controlled. Padinger *et al* [9] reported that J_{SC} and FF were obviously enhanced by annealing the device with an external applied voltage. A latter study by Li *et al* [11] also reported that the device performance was improved by a slowing dry process. These results were related to the better morphology and the increase of the charge carrier mobility.[9,11,12] The same cause should also be responsible for our results. The highest PCE in our experiments is achieved when the annealing temperature is 160 °C which is very close to the annealing temperatures reported by Reyes *et al* [10] and Ma *et al*.[13] Analysis of changes in film morphology has shown that the changes in film crystallinity and aggregation within the film PCBM nanophase lead to improved photovoltaic characteristics at this temperature.[16] When the annealing temperature is increased, a steady enhancement of the open circuit voltage V_{OC} is observed, which is different from the previous results where the values of V_{OC} are almost unchanged at different annealing temperatures. Comparing our experiments with others[9−13] shows that their difference lies in the fact that we use the e-beam evaporated Al rather than the buffer layer and the thermal evaporated Al. Thus it is suggested that the e-beam evaporated Al can induce dipoles in the interface between the active layer and the cathode, which induces the steady enhancement of V_{OC}.

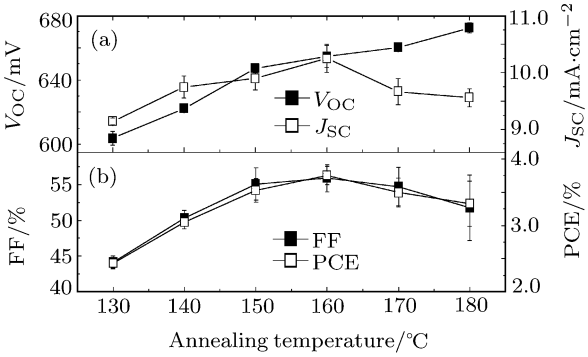


Fig.5. Optimization of glass/ITO/PEDOT:PSS/P3HT:PCBM/Al device, showing the relation between device performance and annealing conditions with P3HT:PCBM layer thickness kept at a constant of 208 nm.

Having been annealed at 160 °C for 10 min, the device shows that V_{OC} reaches about 0.65 V and the PCE is as high as 4.0%. The typical I–V curve is shown in Fig.6. For a solar cell, the characteristic can be described by

$$I = I_0 \left(e^{\frac{q(V+R_s I}{nk_B T}} - 1 \right) + \frac{V - R_s I}{R_{sh}} - I_{ph}, \qquad (1)$$

where I_{ph} is the photocurrent, I_0 is the saturation current of the diode, R_s is the series resistance, R_{sh} is the shunt resistance, q is the electron charge, n is the ideal factor, k_B is the Boltzmann constant, and T is the temperature. By fitting the curve (Fig.6), all the parameters are extracted as listed in Table 1.

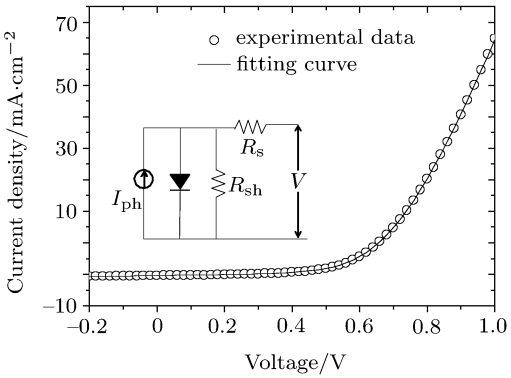


Fig.6. Characteristics of the device around the second optical interference peak, where the data are well fitted by expression (1) and the equivalent circuit of the solar cell is also shown.

Table 1. Parameters extracted from the curve (Fig.6).

parameters	I_{ph}/(mA/cm^2)	I_0/(mA/cm^2)	R_s/(Ω·cm^2)	R_{sh}/(Ω·cm^2)	n
value	10.409	0.00094	3.1	679.7	2.75

4. Conclusions

The effects of optical interference and annealing on device performance are presented. Due to the optical interference effect, J_{SC} shows a periodic behaviour with the variation of thickness. With the help of the simulated results, the first two optical interference peaks are found to be corresponding to thicknesses of 80 and 208 nm. At the same time, the effect of annealing on the performance is also studied. It is found that post-annealing is more favourable than pre-annealing. Based on post-annealing, different annealing temperatures are tested. The optimized annealing condition is 160 °C for 10 min in a nitrogen atmosphere. The device shows that V_{OC} achieves about 0.65 V and the PCE is as high as 4.0% around the second interference peak.

References

[1] Brabec C J, Sariciftci N S and Hummemen J C 2001 *Adv. Funct. Mater.* **11** 15
[2] Yu H Z, Peng J B and Zhou X M 2008 *Acta Phys. Sin.* **57** 3898 (in Chinese)
[3] Zhang C F, Tong S W, Jiang C Y, Kang E T, Chan D S H and Zhu C X 2008 *Appl. Phys. Lett.* **92** 083310
[4] Wang E G, Wang L, Lan L F, Luo C, Zhuang W L, Peng J B and Cao Y 2008 *Appl. Phys. Lett.* **92** 033307
[5] Hou J H, Tan Z A, Yan Y, He Y J, Yang C H and Li Y F 2006 *J. Am. Chem. Soc.* **128** 4911
[6] Sariciftci N S, Smilowitz L, Heeger A J and Wudl F 1992 *Science* **258** 1474
[7] Moulé A J, Bonekamp J B and Meerholz K 2006 *J. Appl. Phys.* **100** 094503
[8] You H L and Zhang C F 2009 *Chin. Phys.* B **18** 349
[9] Padinger F, Rittberger R S and Sarciftci N S 2003 *Adv. Funct. Mater.* **13** 85
[10] Reyes M R, Kim K and Carroll D L 2005 *Appl. Phys. Lett.* **87** 083506
[11] Li G, Shrotriya V, Huang J, Yao Y, Moriarty T, Emery K and Yang Y 2005 *Nature Materials* **4** 864
[12] Mihailetchi V D, Xie H, Boer B D, Popescu L M, Hummelen J C and Blom P W M 2006 *Appl. Phys. Lett.* **89** 012107
[13] Ma W, Yang C, Gong X, Lee K and Heeger A J 2005 *Adv. Funct. Mater.* **15** 1617
[14] Nyuyen L H, Hoppe H, Erb T, Günes S, Gobsch G and Sariciftci N S 2007 *Adv. Funct. Mater.* **17** 1071
[15] Chirvase D, Parisi J, Hummelen J C and Dyakonov V 2004 *Nanotechnology* **15** 1317
[16] Rispens M T, Meetsma A, Rittberger R, Brabec C J, Sariciftci N S and Hummelen J C 2003 *Chem. Commun.* 2116
[17] Peumans P, Uchida S and Forrest S R 2003 *Nature* **425** 158
[18] Hoppe H, Sariciftci N S and Meissner D 2002 *Mol. Cryst. Liq. Cryst.* **385** 233
[19] Dennler G, Forberich K, Scharber M C, Brabec C J, Tomis I, Hingerl K and Fromberz T 2007 *J. Appl. Phys.* **102** 054516